Biometals (2024) 37:389–403
https://doi.org/10.1007/s10534-023-00556-z

RESEARCH

Green synthesis of silver nanoparticles employing hamdard joshanda extract: putative antimicrobial potential against gram positive and gram negative bacteria

Nikhat Firdaus · Ishrat Altaf · Zafar Iqubal · Osama Adeel khan Sherwani · Shamiuddin khan · Mohd Kashif · Bhupendra Kumar · Mohammad Owais

Received: 25 May 2023 / Accepted: 21 October 2023 / Published online: 6 December 2023

Abstract The bio-mediated synthesis of nanoparticles offers a sustainable and eco-friendly approach. In the present study, silver nanoparticles (AgNPs) were synthesized using Joshanda extract, a commercially available herbal formulation derived from a traditional medicinal plant, as a reducing and stabilizing agent. The as-synthesized AgNPs were characterized using UV–Vis spectroscopy, dynamic light scattering (DLS), X-ray Diffraction (XRD) study, and Fourier-transform infrared (FTIR) analysis. UV–Vis spectroscopy exhibited a prominent absorption peak at 430 nm, confirming the formation of AgNPs. DLS analysis revealed the size distribution of the nanoparticles, ranging from 80 to 100 nm, and zeta potential measurements indicated a surface charge of − 14.4 mV. The XRD analysis provide evidence for the presence of a face-centered cubic structure within the silver nanoparticles. FTIR analysis further elucidated the interaction of bioactive compounds from the Joshanda extract with the AgNPs' surface. Strong peaks at 765–829 cm^{-1} indicated C–Cl stretching vibrations of alkyl halides, while the stretching of alkenes C=C was observed at 1641 cm^{-1}. Moreover, the presence of alcohols and phenol (OH) groups was identified at 3448 cm^{-1}, suggesting their involvement in nanoparticle stabilization. The antimicrobial potential of the synthesized AgNPs was evaluated against both gram-negative *Pseudomonas aeruginosa* and gram-positive *Streptococcus mutans* using zone of inhibition assays. The AgNPs exhibited remarkable inhibitory effects against both types of bacteria. Additionally, AgNPs-treated groups demonstrated a significant increase in reactive oxygen species (ROS) levels, indicating potential of as-synthesized AgNPs in disruption of the target microbial membranes. Furthermore, the as-synthesized AgNPs exhibited notable anti-biofilm properties by effectively hindering the development of mature biofilms. This study highlights the efficient green synthesis of AgNPs using Joshanda extract and also provides insights into their physico-chemical properties of as-synthesized nanoparticles. The demonstrated antimicrobial activity against both gram-negative and gram-positive bacteria, along with biofilm inhibition potential, underscores the promising applications of the as-synthesized AgNPs in the field of biomedical and environmental sciences. The study bridges traditional knowledge with contemporary nanotechnology, offering a novel avenue for the development of eco-friendly antimicrobial agents.

N. Firdaus · I. Altaf · Z. Iqubal · S. khan · M. Owais (✉)
Interdiciplinary Biotechnology Unit, AMU, Aligarh, India
e-mail: mdowais2012@gmail.com; owais_lakhnawi@yahoo.com

Present Address:
O. A. k. Sherwani
Consultant Dental Surgeon UPPM, Bulandshahar, UP, India

M. Kashif
Department of Biotechnology, Babasaheb Bhimrao Ambedkar University, Lucknow, India

B. Kumar
Center for Plant Molecular Biology and Biotechnology Division, CSIR- National Botanical Research Institute, Rana Pratap Marg, Lucknow, India

Graphical abstract

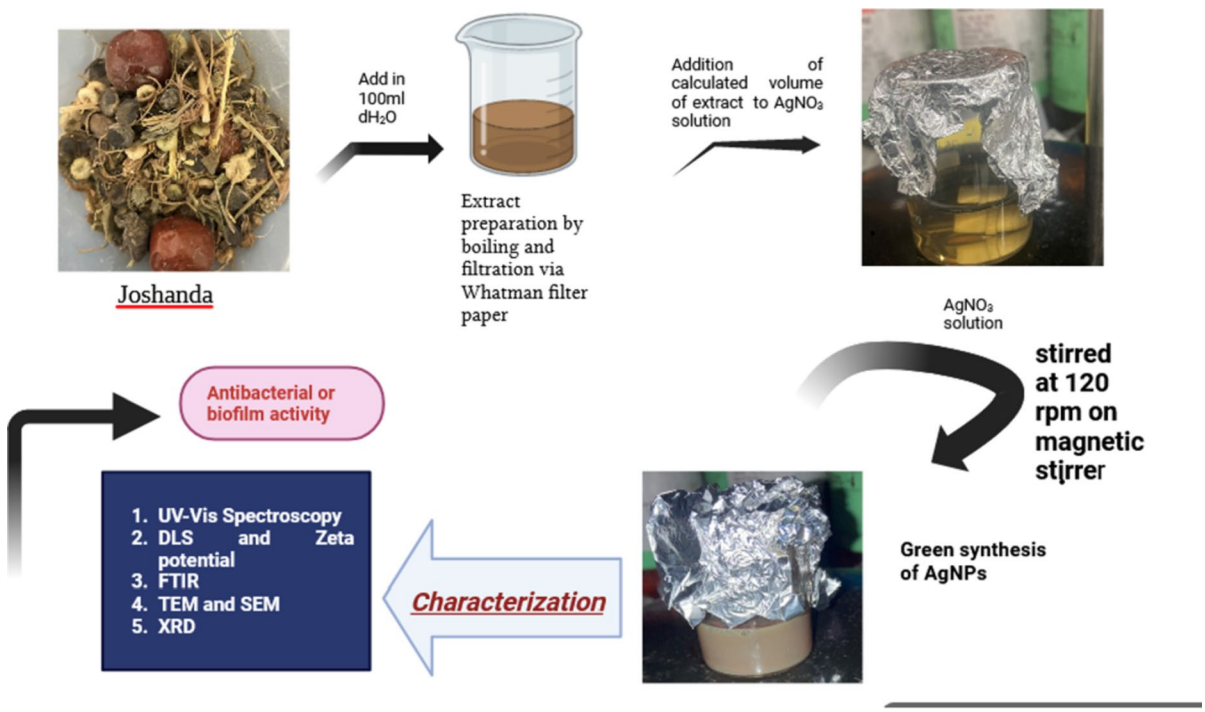

Joshanda Extract -mediated green synthesis of AgNPs (Schematic representation)

Keywords Green synthesis · AgNPs · Joshanda extract · Anti-bacterial · Gram positive · Gram negative bacteria · Biofilm

Introduction

Metallic nanoparticles have remained a focus of interest due to their distinct physicochemical characteristics and wide range of applications in the domains, such as electronics, food, and most greatly in the field of biomedical sciences especially, for their antimicrobial potential and their use as a diagnostic tool (Klebowski et al. 2018; Kumar et al. 2018; Azharuddin et al. 2019; Moutsiopoulou et al. 2019). Among various types of metal nanoparticles, silver nanoparticles (AgNPs) can boast of distinctive physicochemical characteristics that made them suitable for their specific use in the medical field. There are several methods that are widely employed in the fabrication of silver and other nanoparticles. In general, the employment of potentially harmful chemicals and energy-intensive processes in traditional techniques of nanoparticle synthesis not only make them costlier, however, raises questions regarding their influence on the environment (Parashar et al. 2009; Dey et al. 2023). Green synthesis techniques, on the other hand, provide a sustainable and environmentally friendly option for the fabrication of AgNPs by using natural sources such as plant extracts. The organically created AgNPs have several characteristics that make them interesting candidates for innovative medical uses (Oliver et al. 2018).The noble metal-made nanoparticles that are now being examined the most are copper (Moherrer et al. 2012), zinc (Azizi et al. 2014), gold (Gu et al. 2003) and silver. In addition to the aforementioned four, silver nanoparticles have gained a lot of attention in the research area due to their wide range of applications in the field of

microbiology, chemistry, food technology, cell biology, pharmacology, parasitology, and so on (Nour et al. 2019).

Nanoscale silver particles with a high surface-area-to-volume ratio (size below 100 nm) are of particular interest due to their outstanding antimicrobial activity against Gram-positive and Gram-negative bacteria (Morones et al. 2013; Gurunathan et al. 2014) viruses, and other eukaryotic micro-organisms (Gong et al. 2007) when compared to other nanoscale metals. It may also be effective against multidrug-resistant strains, such as *Pseudomonas aeruginosa*, ampicillin-resistant *Escherichia coli*, erythromycin-resistant *Streptococcus pyogenes*, methicillin-resistant *Staphylococcus aureus* (MRSA), and vancomycin-resistant *Staphylococcus aureus* (VRSA) (Rai et al. 2012). Several physical and chemical routes have been used to synthesize AgNPs due to their biocidal properties, and AgNPs have been applied in modifying surfaces, coating, fibre grafting, gel preparations, etc. (Jain et al. 2005; Das et al. 2015).

Traditional roots (physical and chemical methods) of silver nanoparticle synthesis have disadvantages, including the use of toxic precursor chemicals (such as sodium borohydride, potassium bitartrate, methoxypolyethylene glycol, and hydrazine), the use of toxic solvents (such as sodium dodecyl benzyl sulphate and polyvinyl pyrrolidone), and the generation of toxic by-products (Moharekar et al. 2014). In contrast, biological methods (such as plant extract) use fewer toxic reactants and additives. The reaction can occur at room temperature without severe or stringent conditions. The plant extract-based nanoparticles provide low or no cytotoxicity. Consequently, biological methodologies employing plant extracts could be categorized as safe, environmentally friendly, and cost-effective, constituting a viable alternative when applied to microbiology. With the advancement of science, alternative eco-friendly routes have emerged for synthesizing metal nanoparticles (Gurunathan et al 2009).

In the present study we have synthesized silver nanoparticles using simple, cheap and ecofriendly biological synthesis procedure. Joshanda® (Hamdard) extract was used as a reducing and capping agent for the bio-mediated conversion of silver salts into silver nanoparticles. A well-known herbal cure in Unani medicine called Hamdard Joshanda has been used for generations to treat a variety of respiratory conditions. Joshanda, which translates to "brew,"is a mixture of numerous medicinal herbs recognized for their curative qualities. The Joshanda decoction exhibits an identifiable accumulation of saponins, alkaloids, and sterols. This concoction has notable antibacterial qualities, especially when it comes to microorganisms linked to URIs (upper respiratory tract infections). Furthermore, its powerful antioxidant activity implies its potential for treatments in respiratory ailments (Khan et al., 2015). However, the main components are frequently dried extracts or powders of medicinal herbs like basil leaves (Ocimum basilicum), liquorice root (Glycyrrhiza glabra), cinnamon bark (Cinnamomum verum), ginger rhizome (Zingiber officinale), and black pepper (Piper nigrum). The exact composition may vary depending on the manufacturer. So one of the main important reasons to choose Joshanda extract as our reducing agent is that it is a natural remedy, made from plant-based ingredients, and does not contain any artificial additives or chemicals. It is generally considered safe for consumption by individuals of different age groups, including children and the elderly.

Pseudomonas aeruginosa and *Streptococcus mutans* bacterial isolates were used to establish antimicrobial potential of as-synthesized AgNPs nanoparticles.

Experimental procedure

Materials

We procured microbiological culture media including Luria Broth (LB), Brain Heart Infusion (BHI), and Agar (India). The source of silver nitrate was Merck Research Laboratories Private Limited. *Pseudomonas aeruginosa* and *Streptococcus mutans* bacterial isolates were obtained from the Institute of Microbial Technology (IMTech), Chandigarh, India. FITC, DCFH-DA, SYTO9, and PI dye for fluorescence microscopy were purchased from Sigma-Aldrich (St. Louis, MO) Utilizing Nutrient Broth and Brain Heart Infusion, standard strains were sub-cultured. The colonies of the bacterial strains were stored in glycerol (20%) at − 20 °C.

Preparation of joshanda extract

Hamdard Joshanda, a blend of therapeutic herbs, is commonly consumed as a natural remedy for various ailments. According to Unani medical theory, respiratory disorders are an excess of coldness and phlegm in the body's humoral system. It is believed that Joshanda might fix these discordances and bring about equilibrium in the body.

A known amount (60 g) of Joshanda ingredients was boiled in 100 ml of distilled water for a specified duration till the volume of the solution gets halved of the original. The resulting herbal infusion was then subjected to pass through Whatman filter paper (Iravani et al. 2013) to get rid of any solid particulates and obtain a clear solution. The extract was finally stored at − 20 °C for further use.

This herbal extract was employed as both a reducing and a stabilizing agent for the synthesis of silver nanoparticles. The reduction process was visually monitored as the color of the silver nitrate solution changed from pale yellow to dark brown. The color change was indicative of the formation of silver nanoparticles.

Biosynthesis of silver nanoparticles (AgNPs)

During the process of biosynthesizing silver nanoparticles (AgNPs), a carefully measured 5 mL volume of the previously prepared Joshanda extract(Aqueous based) and an equal volume of the 0.1 mM $AgNO_3$ solution were combined to yield the silver nanoparticles. The amalgamated solution was added to a glass beaker, which was placed on a magnetic stirrer and continuously stirred. The solution was elevated to a regulated temperature of between 30 and 35 °C with the magnetic stirrer set to run at 120 rpm. A slow transformation of the solution was initiated by this carefully timed interaction of heat and agitation, as seen by the changing color of the solution from its initial pale color to a distinctive brown hue (Fig. 1).

Characterization of AgNPs

UV–visible spectroscopy

UV–visible spectroscopy is a technique used to analyze the absorption and transmission of light in the ultraviolet (UV) and visible regions of the electromagnetic spectrum. On a double-beam spectrophotometer (Shimadzu) with a resolution of 1 nm in the range of 200–800 nm, the ultraviolet–visible (UV) spectrum of as-prepared AgNPs nanoparticles was recorded. The reaction mixture was also monitored at different time intervals using UV–Vis spectroscopy to assess the evolution of the nanoparticles. The

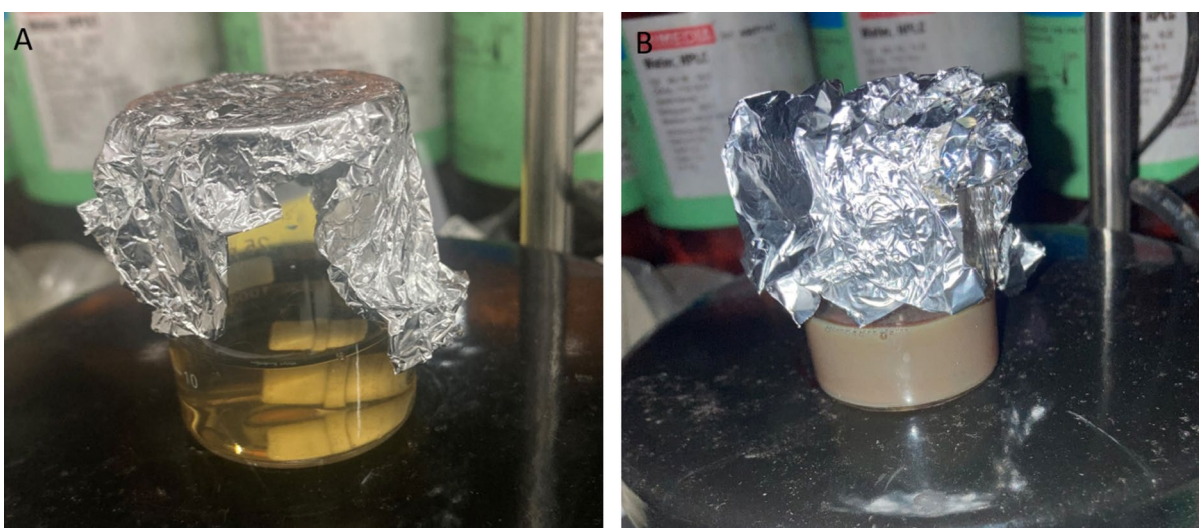

Fig. 1 Illustrates the process of green synthesis of AgNPs (**A**) Pale yellow mixture representing the initial stage of the synthesis process where $AgNO_3$ and Joshanda extracts are combined. (**B**) Brown colored mixture indicates the successful formation of AgNPs. (Color figure online)

absorbance spectra were recorded in the range of 200 to 800 nm.

Electron microscopic studies

Using TEM and SEM techniques, the size dimensions and surface morphology of the nanoparticles were characterized. A sample was prepared by depositing a drop of reactant product on a 200-mesh copper grid and then covering it with a carbon-stabilized formvar film for probing the as-synthesized AgNPs. As a negative stain, uranyl acetate (2%w/v) was used. Before TEM analysis, the sample was drained of superfluous fluid. JEOL-brand electron microscope was utilized for TEM analysis. For surface morphological characterization of the as-synthesized AgNPs JEOL's JSM67500F was used for scanning electron microscopy (SEM).

Dynamic light scattering (DLS)

Dynamic Light Scattering (DLS, using Dynpro-Tc-04 instrument; Protein Solution, Wyatt Technology, Santa Clara, CA) was implemented to measure the diffusion of dispersed particles for the size analysis of the nanoparticles. Using the Stokes–Einstein equation, the average hydrodynamic diameter was determined. At 90° from the incident beam, the dispersed light intensity was measured. In the default analysis approach, the data was analyzed. For determining the size of the as-synthesized AgNPs the mean value of 10 runs (performed in triplicate) was considered.

FTIR spectroscopy

Fourier Transform Infrared Spectroscopy (FTIR) was utilized to analyze the molecular composition and structure of a sample. FTIR spectroscopy provided valuable information about the functional groups present in the as- synthesized nanoparticles by measuring the absorption and transmission of infrared radiation. It is a versatile technique used in various fields, including chemistry, pharmaceuticals, materials science, forensics, and environmental analysis. FTIR can identify chemical bonds, characterize unknown substances, detect impurities, monitor chemical reactions, determine sample purity, and aid in the understanding of molecular interactions.

X – ray diffraction (XRD) analysis

Following centrifugation operations at 5000 g for 20 min, the resultant silver nanoparticle pellet was dispersed in 10 ml of deionized water to yield the purified silver nanoparticle solution. Subsequently, the purified silver nanoparticles were subjected to freeze-drying. The structural and compositional analysis of these dried silver nanoparticles was carried out via X-ray diffraction (XRD) with a Rigaku RINT 2100 series instrument. Employing an X'Pert Pro X-ray diffractometer that ran at 40 kV and 30 mA and used Cu K radiation in a -2 configuration, the dried mixture of silver nanoparticles was investigated for Ag nanoparticle production.

The assessment of the MIC of as-synthesized AgNPs against bacterial pathogens

The Minimum Inhibitory Concentration (MIC) assay of a given antibacterial agent against bacterial pathogens is crucial for determining the effectiveness of as-developed antimicrobial agents. The MIC test involves exposing the bacterial strain to various concentrations of the antimicrobial agent and observing the lowest concentration that inhibits visible growth. The MIC value of the as-synthesized aqueous based AgNPs nanoparticles was determined via the micro-dilution method against the investigated bacterial strains *Pseudomonas aeruginosa* and *Streptoococcus mutans* provided by Institute of Microbial Technology (IMTech), Chandigarh, India. The MIC was estimated by employing 96 well micro-dilution plates performed based on viability test.

Antimicrobial potential of as-synthesized AgNPs was determined by the agar well diffusion method

The antimicrobial activity of as-synthesized aqueous based AgNPs was also assessed using the agar well diffusion technique. A 100 µl aliquot of the suspended culture was evenly spread on the petri dish with a sterile plastic spreader and incubated at 37 °C. After one hour of incubation, wells were drilled into the agar plate. Subsequently, an increasing amount of as-synthesized AgNPs (1 mg/ml stock solution) or standard antibiotic was dispersed into the wells of a particular agar plate. The combination of antimicrobial potential of nanoparticles and antibiotics was

also investigated. After 24 h, the zone of inhibition was determined by measuring the clear region surrounding each well, which corresponded to the bacterial clearance mediated by AgNPs.

Assessment of biofilm disruption (XTT)

XTT (2, 3-bis (2-methoxy-4-nitro-5-sulphophenyl)-2H-tetrazolium-5-carboxanilide) assay was conducted for a comprehensive assessment of biofilm disruption against *Pseudomonas aeruginosa* with slight modifications as previously reported method (Saigal et al. 2019). Briefly, 100 µl of sterile liquid broth was poured in each well of 96 –well micro titer plate, inoculated with the desired bacterial strains and incubated at 37 °C for 24 h to allow biofilm formation. Next biofilm of *P. aeruginosa* was exposed to standard antibiotics, ranging from low to high concentrations. The potential of synergistic effect of silver nanoparticles (AgNPs) and standard antibiotic was also investigated. The biofilms of the same strains were exposed to varying concentrations AgNPs (alone) and their combination with antibiotics. The biofilm harboring culture plates were incubated for 24 h at 37 °C. After incubation, each well was subjected to 50 µl of XTT salt solution (HiMedia) and the plate was further incubated in the dark for 90 min at 37 °C. Bacterial dehydrogenase converts XTT tetrazolium salt to XTT formazan, which ensues in a colorimetric change (turns orange) that in turn can be correlated with cell survival. These colorimetric variations were determined by taking their optical densities at 490 nm on a spectrophotometer. The % inhibition data was further interpreted from dose – response curves.

The XTT analysis enabled us to quantify the biofilm disruption achieved through these combined treatments, providing insights into the potential synergistic interactions and the optimal combination ratios for maximal biofilm eradication.

Confocal laser scanning microscopic analysis (CLSM)

The biofilm is a structured community of microorganisms, such as bacteria, fungi, algae, or protozoa that are embedded within a self-produced matrix of extracellular polymeric substances (EPS*). P. aeruginosa* was cultured in 30 ml of nutrient broth medium at 37 °C overnight. An aliquot of a log phase bacterial culture (containing 10^6 cfu/ml) was suspended in 30 ml of broth and a drop of 5 µL dispensed onto a sterile coverslip placed in the 6 well microtiter plate. The setup was incubated for 24 h at 37 °C in the incubator without shaking enclosed in the aluminum foil to promote the growth of mature biofilm. Afterward, the mature biofilm was washed and subjected to 100 µL as synthesized AgNPs (from 1 mg/ml stock solution) and then was incubated for next 3–5 h at 37 °C and after that the coverslips were fixed with 4% PFA followed by washing the cells after incubation of 30 min and finally the cells were stained with FITC dye. Fixed coverslips were washed thrice with sterile PBS to remove unbound FITC dye. The FITC dye was excited at 488 nm and was monitored at its emission spectra 519 nm under Confocal Laser Microscope. Both the control and treated samples were prepared via the same procedure and observed under CLSM.

Detection of intracellular ROS production by as synthesized AgNPs nanoparticles

Due to their distinct physical and chemical characteristics, interactions with biological systems, and ability to generate ROS, nanoparticles have drawn a lot of attention. The generated ROS was measured by employing a fluorescence-based assay via ROS-sensitive dye as 2, 7-dichlorofluorescin diacetate (DCFH-DA). DCFH-DA undergoes intracellular deacetylation by esterases that results in the formation of 2, 7-dichlorofluorescin (DCFH). DCFH is a non-fluorescent, relatively stable compound within cells. DCFH is promptly oxidized and converted to the highly fluorescent compound 2, 7-dichlorofluorescein (DCF) in the presence of reactive oxygen species (ROS). ROS, specifically hydrogen peroxide (H_2O_2) and hydroxyl radicals (OH), oxidize DCFH to produce DCF and water. The log phase bacteria ((10^6 CFU/m) were washed thrice with fresh medium. DCFH-DA was incubated with bacterial culture for 30 min at 37 °C at shaking. The unbound DCFH-DA was extracted via centrifugation at 15000xg while washing with sterile PBS. For substantiation of as-synthesized AgNPs ROS generation, treated bacterial cells were observed under Zeiss fluorescence microscope (United States). The higher fluorescence intensity corresponds to the increased production of reactive oxygen species.

Statistical analysis

Data were analyzed by one way and two way ANOVA to assess the differences among groups. Statistical calculations were performed via GraphPad Prism version 8. Significance was indicated as ***p-value ≤ 0.001, ** p-value ≤ 0.01 and * p-value ≤ 0.05. Experiments were performed in triplicates.

Results

UV visible spectroscopy

Post exposure to electromagnetic radiations, electrons in the conduction band typically oscillate resonantly between materials with positive and negative permittivity. Surface plasmon resonance results from the localized electron oscillation in metal nanoparticles, which set characteristics features post their creation. We followed the reduction of silver ions into bio-synthesized nanoparticles employing UV–Vis spectroscopy. All the related solutions (used in fabrication of AgNPs) were scanned from 200 to 800 nm of light. The ability of Joshanda extract to facilitate the development of monometallic nanoparticles established. In contrast to the silver nitrate solution (which fails to absorb at 430 nm), Ag nanoparticles displayed a distinctive spectra with a clear peak at characteristic wavelength (Fig. 2). After $AgNO_3$ solution was treated with Joshanda extract, we observed change in the colour (from pale yellow to dark brown). The transformation of silver ions (Ag^+) into silver nanoparticles and the colour change have been reported to be linked to one another.

Kinetics of AgNPs synthesis upon incubation of silver nitrate solution with joshanda extract

The Joshanda extract mediated time kinetics of AgNPs synthesis exhibited distinct stages of nanoparticle evolution. At the initial stage (0 h), no noticeable peak was observed in the UV–Vis spectrum, indicating the lack of synthesized nanoparticles. However, after 30 min, a distinct peak emerged at 430 nm, signifying the onset of AgNP formation. This spectral feature suggested the presence of smaller-sized nanoparticles, which gradually accumulated over time (Fig. 3).

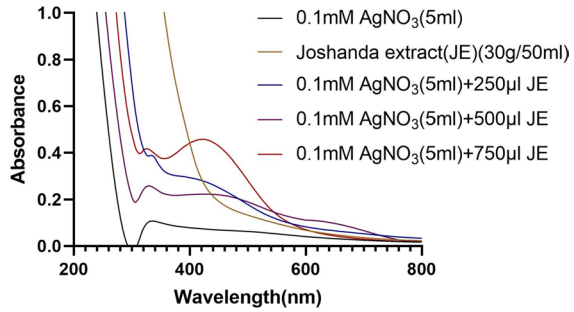

Fig. 2 UV–visible spectrum of as-synthesized AgNPs fabricated employing increasing amount of Joshanda extract

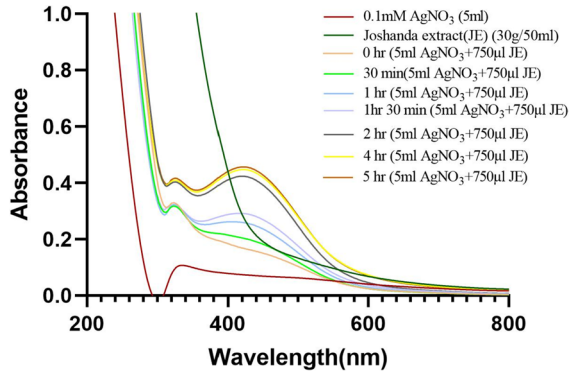

Fig. 3 Time-dependent kinetics of AgNP synthesis from silver nitrate in the presence of Joshanda extract

Surprisingly, the subsequent time points, namely 2, 4, and 5 h, showed consistent peaks at 430 nm, with escalating intensities (Fig. 3). This intriguing observation indicated that the synthesis process had stabilized by the 2-h time point, and the size distribution of the nanoparticles had reached a relatively steady state.

Electron microscopic study

The shape of the as-synthesized AgNPs was determined by SEM analysis. The SEM image revealed the shape of as synthesized nanoparticles to be spherical and uniform size distribution. TEM analysis revealed the size of as-synthesized nanoparticles to be in the range of 40–80 nm (Fig. 4).

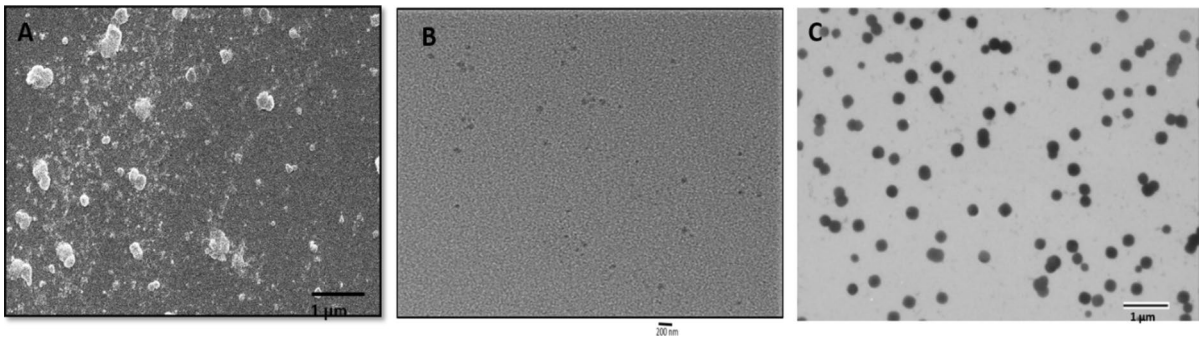

Fig. 4 Shape and size analysis of as-synthesized AgNPs: (**A**) SEM analysis image depicting the shape of as-synthesized AgNPs (**B**) TEM analysis at 500 X, (**C**) TEM at 1000 X

Dynamic light scattering (DLS)

The Dynamic Light Scattering investigation revealed that the size of as-synthesized nanoparticles was in the range between 80 and 100 nm in size (Fig. 5). DLS size measurements typically show larger size dimensions as compared to the dimensions determined by TEM investigation. While Dynamic Light Scattering (DLS), which measures particle dimensions after being dispersed in a specific medium, with stern layer around each particle, in contrast, TEM examination offers information about the size and shape of individual nanoparticles after particle being dried under high vacuum. DLS analysis also revealed the value of zeta potential to be -14.4 mV which confirms the stability of the as-synthesized nanoparticles**.** The polydispersity index (PDI) was found to be 0.354 found employing DLS.

FTIR spectroscopy-based functional group identification in AgNPs

Based on how different materials interact with infrared radiation, FTIR spectroscopy, also known as Fourier Transform Infrared Spectroscopy, is a potent analytical technique for identifying and characterizing the chemical composition of various substances. Based on how different materials interact with infrared radiation, FTIR spectroscopy, also known as Fourier Transform Infrared Spectroscopy, is a potent analytical technique for identifying and characterizing the chemical composition

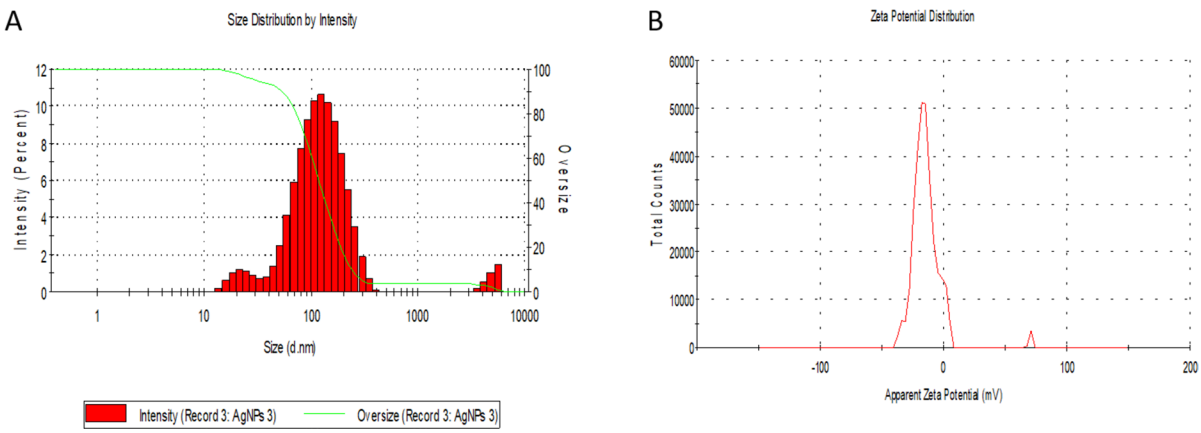

Fig. 5 Size analysis of the as-synthesized AgNPs as determined by DLS analysis. Dynamic Light Scattering (DLS) based particle size analysis suggested overall particle diameter of the as-synthesized AgNP nanoparticles to be approximately in the range 80–100 nm. The stability was confirmed as the apparent zeta potential was found to be − 14.4 mV

of various substances. In order to characterize the functional groups present in the as-synthesized nanoparticles, FTIR spectroscopy was conducted. The presence of various chemical (Fig. 6) groups gave rise to specific peaks corresponding to various wave number. We found C–Cl stretching vibrations of alkyl halides corresponding to strong peaks at 765–829 cm^{-1}, stretching of alkenes C=C at 1641 cm^{-1} and stretching of alcohols and phenol (OH) groups at 3448 cm^{-1} on the surface of nanoparticles. It can be concluded that the nanoparticles were coated by the alkyl halides, alkenes and alcohol groups present in the Joshanda extract. The extract's biomolecules may adhere to the surface of nanoparticles and give them stability, preventing aggregation.

X-ray diffraction (XRD) analysis

The X-ray diffraction study of the crystallinity of the biologically synthesized silver nanoparticles revealed a different pattern. This pattern had five distinct peaks and diffraction lines that were clearly visible at angles of 2=32.24, 38.46°, 44.56°, 64.25°, and 78.14°. These angles indicated the existence of a face-centered cubic structure in the silver nanoparticles, which were indexed as 111, 122, 200, 220, and 311 corresponding to the respective angles (Fig. 7)**.**

Evaluation of as-synthesized AgNPs' MIC against bacterial strains

The minimum inhibitory concentration (MIC) of as-synthesized AgNPs was determined to be 125 µg/ml. In addition, we found that our as-synthesized AgNPs had a synergistic effect when combined with the conventional antibiotic streptomycin. When 100 µl of streptomycin (1 mg/ml stock) was added to 100 µl of as-synthesized AgNPs, the MIC against the gram-negative strain *Pseudomonas aeruginosa* was determined to be 64 µg/ml. We also performed the same MIC test against the gram-positive strain *Streptoococcus mutans* and determined that the MIC was 64 g/ml with AgNPs alone and 32 g/ml with the standard antibiotic; however, the MIC with the standard antibiotic alone was 250 µg/ml for both *Pseudomonas aeruginosa* and *Streptoococcus mutans.* As a result, it was determined that the MIC value decreases dramatically when treated with AgNPs (Table 1).

Antimicrobial potential of as-synthesized AgNPs was determined by the agar welll diffusion method

The zone of inhibition assay provides confirmatory anti-microbial potential of AgNPs against the bacterial and fungal strains (Fig. 8). The bactericidal effect of nanoparticles can be attributed to the combined antimicrobial effects (Jain et al. 2009) possessed by 'Nano-silver' and Joshanda extract. The

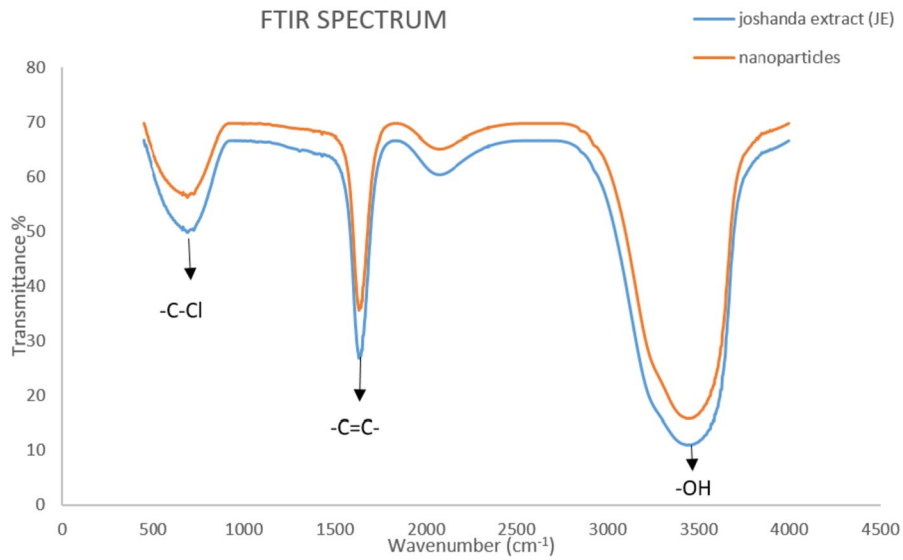

Fig. 6 FTIR spectrum of as-synthesized AgNPs: FTIR spectra of as-synthesized AgNPs generated after incubation of Hamdard joshanda extract with aqueous solution of $AgNO_3$.The blue curve represents pure joshanda extract, and the orange curve corresponds to as-synthesized AgNPs. (Color figure online)

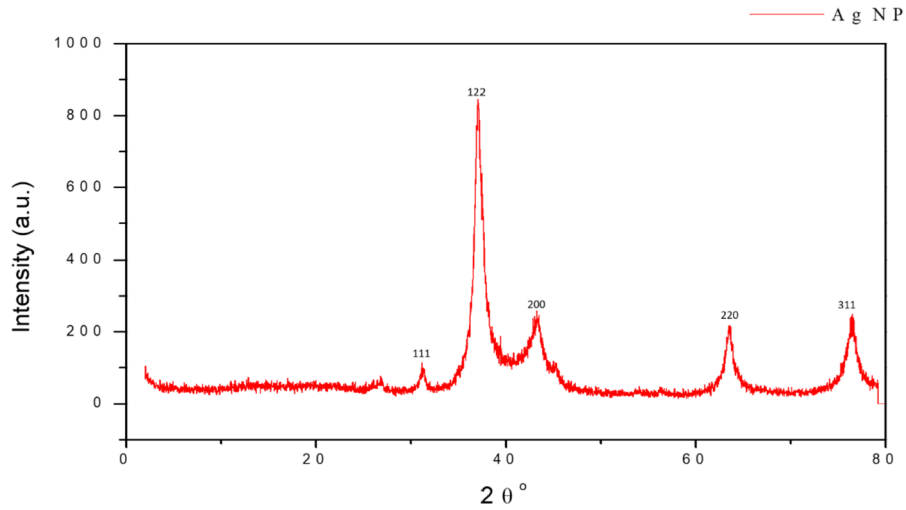

Fig. 7 The X-ray diffraction (XRD) pattern illustrates the structural characteristics of silver nanoparticles (AgNPs) prepared through the reduction of silver ions using Joshanda extract. The peaks observed in the XRD pattern correspond to the crystallographic planes of the AgNPs

Table 1 Comparison of MIC values of nanoparticles against gram negative and gram positive bacterial strains

Groups	Minimum inhibitory concentration	
	P. aeruginosa	*S. mutans*
AgNPs alone	125 µg/ml	64 µg/ml
AgNPs + antibiotic	64 µg/ml	32 µg/ml
Antibiotic alone	250 µg/ml	250 µg/ml

nanoparticles might lower the cell-to-cell interaction while the internalization of nanoparticles in bacteria induces ROS production. This, in turn, affects DNA and total cellular machinery, thereby killing the microbial cells.

Assessment of biofilm (XTT)

The XTT method was employed for assessment of biofilm inhibition. The cultured cells were treated with different formulations, such as, antibiotic, nanoparticles, and antibiotic + nanoparticles combination.

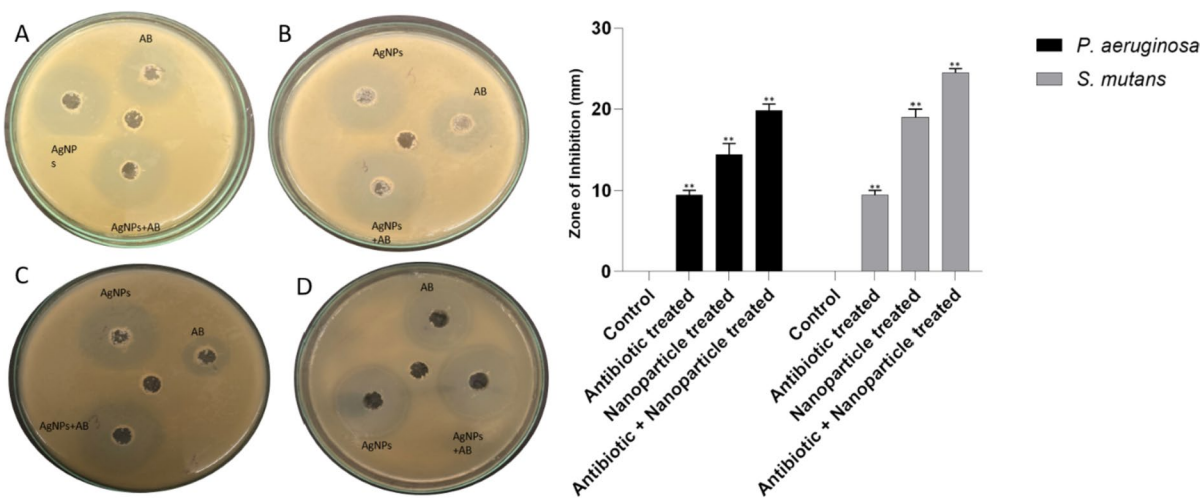

Fig. 8 Antimicrobial potential of as-synthesized AgNPs as expressed in terms of the zone of inhibition (in mm) in background of standard antibiotic. **A**, **B** corresponds to *P.aeruginosa* and **C**, **D** to *S.mutans*. The results are shown as (the mean standard deviation) ± SD; ** p-value ≤ 0.01. The experiments were repeated three times

From the data shown, it was conferred that antibiotic alone and nanoparticles alone significantly inhibited the biofilm formation as compared to PBS that was administered to control wells. In addition, the formulation of antibiotic+nanoparticles contributed synergistically to biofilm inhibition. The antibiotic + nanoparticles treatment showed more significant biofilm inhibition than antibiotic alone, nanoparticles alone, or the control group (Fig. 9).

Detection of intracellular ROS production by as-synthesized AgNP nanoparticles

Assessment of the ROS production was done via treatment of AgNPs by utilizing fluorescence dye, DCFH-DA (Fig. 10**).** In general, nanoparticles induce the generation reactive oxygen species (ROS) which is being detected by the DCFH-DA dye. DCFH-DA is a cell-permeable compound that is hydrolyzed by intracellular esterases to form DCFH, which can be oxidized by ROS to yield the highly fluorescent DCF. By measuring the intensity of DCF fluorescence, researchers can quantitatively assess ROS levels within the cells. As shown in Fig. 10, a significant increase in DCF fluorescence was observed upon the treatment of as-synthesized AgNPs.

Inhibition of biofilm (CLSM)

The biofilm inhibition assay was performed to confirm the anti-biofilm activity of the as synthesized AgNP nanoparticles. There was abundant biofilm

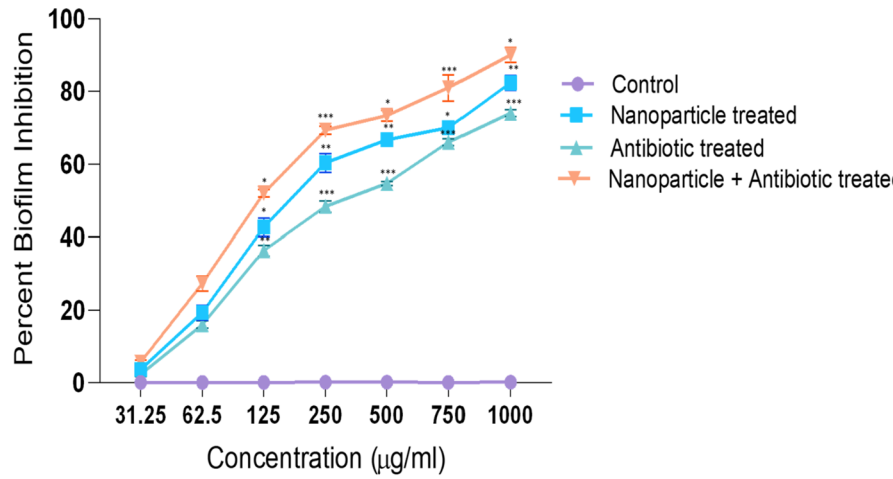

Fig. 9 Percent biofilm disruption by XTT assay in *P. aeruginosa***.** The results are shown as (the mean standard deviation) ± SD; *** p-value ≤ 0.001, ** p-value ≤ 0.01 and * p-value ≤ 0.05. The experiments were repeated three times

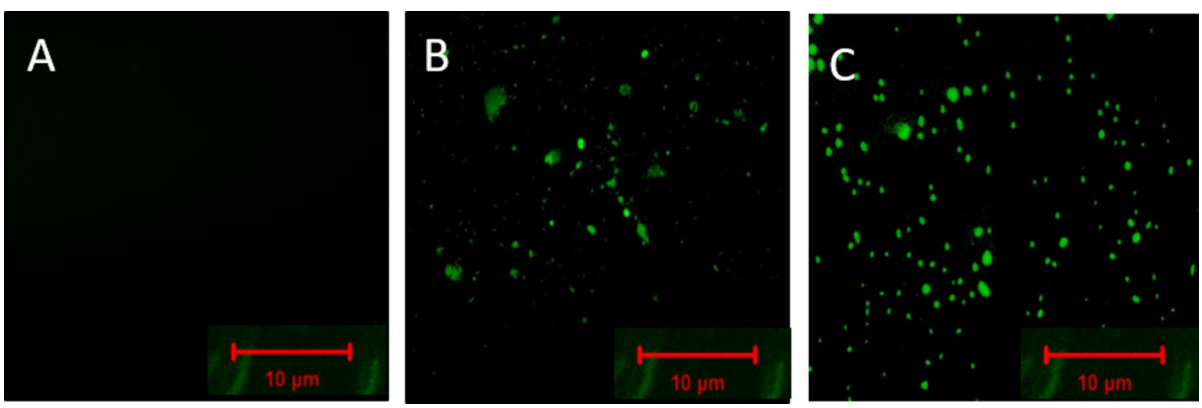

Fig. 10 Generation of ROS upon the treatment of as-synthesized AgNPs. Micrograph (**A**) fluorescence micrograph showing untreated live cells, (**B**) micrograph showing the effect of as generated ROS upon treatment of standard antibiotic (**C**) micrograph showing intensifying effect of ROS upon treatment of AgNPs (125 µg/ml)

development as a result of unrestricted control cell growth. However, as seen in Fig. 11, treatment with AgNPs prevented the development of biofilm.

Discussion

Due to its environmental friendliness, cost effectiveness, better biocompatibility, improved characteristics, and alignment with sustainable development goals, the green synthesis of nanoparticles is taking centrestage. Green synthesis techniques result in the fabrication of the biocompatible nanoparticles, minimize production costs, display comparable or improved qualities. Additionally, the applied bio-mediated technique avoids the use of hazardous chemicals or high-temperature-based reduction conditions, making the entire process more economical and environmentally benign (Tran et al. 2013). In the present study we have synthesized silver nanoparticles using Hamdard Joshanda extract as a reducing and stabilizing agent. To follow the synthesis of AgNPs, spectrophotometric UV–VIS analysis was performed. In accordance to a UV- absorption spectrophotometric investigation, monometallic silver nanoparticles were synthesized with a maximum peak at 430 nm (Fig. 2). The FTIR analysis showed the presence of various functional groups such as alkyl halides, stretch of alkenes, and phenol and alcoholic groups that were present in both Joshanda extract and as synthesized AgNPs. This explicitly suggest the role of joshanda extract in nanoparticles fabrication. The size of the nanoparticles was in the range of 80–100 nm as revealed through DLS.The TEM analysis suggested the size dimension in the range of 40–80 nm. The discrepancy in the observed average size of the as-synthesized particles determined by the above specified two different methods can be attributed to the technique used in size determination (Wang et al. 2017).

The antimicrobial potential of the as-synthesized AgNPs was assessed against both Gram-negative and Gram-positive bacterial strains. The antimicrobial effect of AgNPs alone and in combination with standard antibiotic was also compared. Agar well diffusion assay further confirmed the antimicrobial

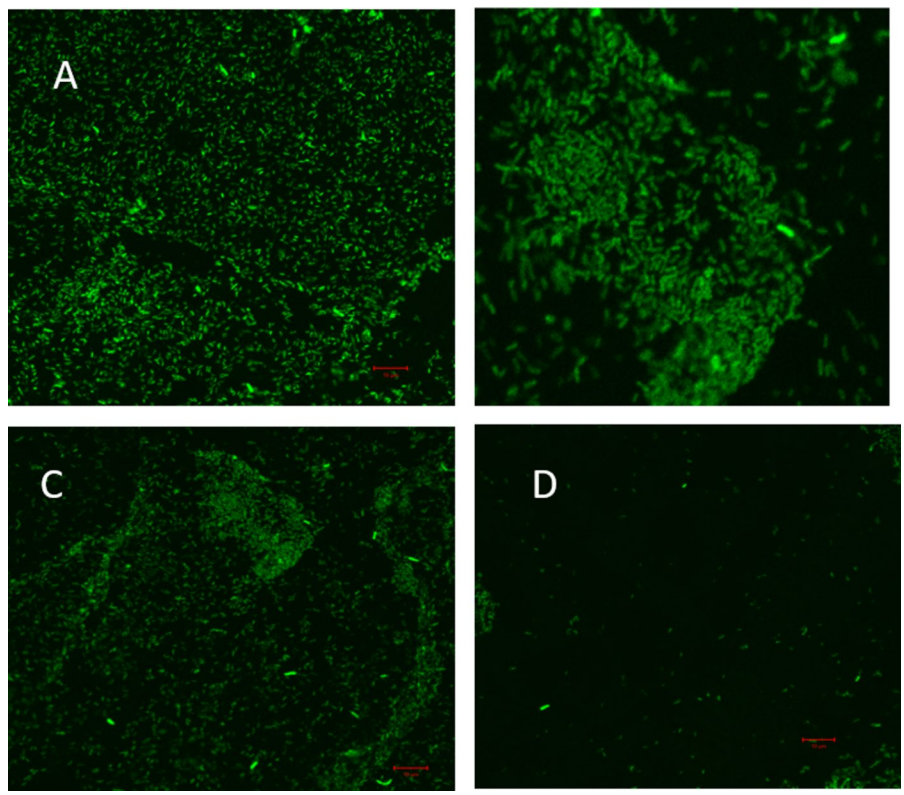

Fig. 11 Inhibition of *P. aeruginosa* biofilm by as-synthesized AgNPs. (**A**) Mature biofilm formation by *P. aeruginosa* (**B**) Inhibition of biofilm by the treatment of antibiotic (**C**) Inhibition of biofilm by the treatment of AgNPs (**D**) Inhibition of biofilm by the treatment of AgNPs + antibiotic

potential as evident by the clear zone of inhibition (Fig. 8). Interestingly, the combination demonstrated outstanding antibacterial potential against bacterial isolates that did not respond to treatment with antibiotics alone. This suggests that as-synthesized AgNPs can be used as alternative antimicrobial agent against drug resistant microbial strains as well. We examined the antibacterial efficacy of as-synthesized nanoparticles against bacterial isolates that were both susceptible and resistant. The bacterial isolates employed in the current study were generally responsive to various antibiotic classes. Some isolates, though, exhibited resistance to a particular class of antibiotics. For instance, *P. aeruginosa*, one of the several bacterial isolates included in the study, did not respond to ampicillin alone.

After establishing antimicrobial potential against sensitive as well as resistant isolates, we attempted to identify a plausible operational mechanism responsible for observed antimicrobial activity. It was observed that as-synthesized AgNPs induced ROS generation (Fig. 10). The ROS generated by nanoparticles affected the proteins, DNA, and lipids of the treated cells, resulting in their eventual demise. ROS production was found to be directly proportional to AgNPs concentration.

A biofilm is a structured community of microorganisms, such as bacteria, fungi, algae, or protozoa, encased in an extracellular polymeric substance (EPS) matrix. Biofilms can form on a variety of surfaces, such as biological tissues, medical devices, industrial equipments, and natural environments such as rocks and submerged surfaces. When individual microorganisms adhere to a surface and begin to multiply, biofilms form. The microorganisms secrete EPS, which forms a protective and adhesive matrix, as their population increases. The EPS matrix provides structural stability and aids in anchoring the biofilm to the surface. It also facilitates communication and cooperation among the biofilm's microorganisms. Compared to their planktonic (free-floating) counterparts, biofilm-dwelling microorganisms exhibit distinctive characteristics. They endure alterations in gene expression, metabolism, and behavior that can improve their survival and resilience. Frequently, biofilms exhibit enhanced resistance to antimicrobial agents, immune responses of the host organism, and other environmental stresses. Interestingly, as-synthesized AgNPs also showed strong anti-biofilm potential against *Pseudomonas aeruginosa* biofilm.

The proposed bio-mediated synthesis of AgNP nanoparticles is a promising method for the efficient, cost-effective, and non-toxic production of nanoparticles at scale. This may have enormous scope and application in the pharmaceutical industry. The efficacy of silver nanoparticles against drug-resistant bacterial strains makes them a promising alternative to currently available antibiotics in the fight against the resistance threat. Fascinatingly, the potential of nanoparticles to create ROS may also find use in the elimination of cancerous cells.

Conclusion

In conclusion, the present study offers a successful green synthesis approach for AgNPs using Joshanda extract. The synthesized AgNPs exhibited a characteristic UV–Vis absorption peak at 430 nm and a size distribution ranging from 80 to 100 nm, as determined by DLS analysis. The FTIR analysis provided insights into the functional groups involved in the synthesis and stabilization of AgNPs. Furthermore, the AgNPs displayed significant antimicrobial activity, as demonstrated by the zone of inhibition, ROS detection, biofilm inhibition, and MIC determination assays. These findings highlight the potential of AgNPs synthesized from natural herbal extracts as effective antimicrobial agents in various applications.

The time kinetics of silver nanoparticle synthesis using Joshanda extract displayed a well-defined progression, from the absence of nanoparticles to the emergence of a characteristic peak at 430 nm within 30 min. Subsequent time points demonstrated consistent peak positions at 430 nm with increasing intensities, indicative of nanoparticle growth and stabilization. This study sheds light on the controlled synthesis process of AgNPs using natural extracts, offering valuable insights for the development of green and sustainable nanoparticle synthesis methods. Further research could explore the optimization of synthesis parameters to tailor the nanoparticle characteristics for their specific applications specifically in treatment against drug resistant bacteria.

Acknowledgements The authors express their gratitude to the Coordinator of the Interdisciplinary Biotechnology Unit, Aligarh Muslim University, Aligarh, for providing us with the facilities to complete this study.

Author contributions NF and MO: conceived and designed the experiments. NF: performed all the experiments IA, ZI, SK, MK, BK and OS: helped in the same. MO: contributed all the reagents, materials, and analysis tools used in the experiment. NF: wrote the first draft of the manuscript.

Funding We did not receive any funding from any agency for this work.

Data availability All datasets generated for this study are included in the article.

Declarations

Conflict of interest The authors declare no conflict of interest.

References

Azharuddin M, Zhu GH, Das D, Ozgur E, Uzun L, Turner AP et al (2019) A repertoire of biomedical applications of noble metal nanoparticles. Chem Commun 55:6964–6996. https://doi.org/10.1039/C9CC01741K

Azizi S, Ahmad MB, Namvar F, Mohamad R (2014) Green biosynthesis and characterization of zinc oxide nanoparticles using brown marine macroalga Sargassum muticum aqueous extract. Mater Lett 1(116):275–277

Das A (2015) Preparation and characterization of silver nanoparticle loaded amorphous hydrogel of carboxymethylcellulose for infected wounds. Carbohydr Polym 130:254–261

Dey G, Patil MP, Banerjee A, Sharma RK, Banerjee P, Maity JP, Singha S, Taharia M, Shaw AK, Huang HB, Kim GD, Chen CY (2023) The role of bacterial exopolysaccharides (EPS) in the synthesis of antimicrobial silver nanomaterials: a state-of-the-art review. J Microbiol Methods 17:106809. https://doi.org/10.1016/j.mimet.2023.106809. (**PMID: 37597775**)

Gong P, Li H, He X, Wang K, Hu J, Tan W, Zhang S, Yang X (2007) Preparation and antibacterial activity of Fe3O4@Ag nanoparticles. Nanotechnology 18(28):285604

Gu H, Ho PL, Tong E, Wang L, Xu B (2003) Presenting vancomycin on nanoparticles to enhance antimicrobial activities. Nano Lett 3(9):1261–1263

Gurunathan S, Han JW, Kwon DN, Kim JH (2014) Enhanced antibacterial and anti-biofilm activities of silver nanoparticles against Gram-negative and Gram-positive bacteria. Nanoscale Res Lett 9(1):1–7

Gurunathan S, Kalishwaralal K, Vaidyanathan R, Venkataraman D, Pandian SR, Muniyandi J, Hariharan N, Eom SH (2009) Biosynthesis, purification and characterization of silver nanoparticles using Escherichia coli. Colloids Surf, B 74(1):328–335

Iravani S, Zolfaghari B (2013) Green synthesis of silver nanoparticles using Pinus eldarica bark extract. Biomed Res Int. https://doi.org/10.1155/2013/639725. (**PMID: 24083233**)

Jain D, Daima HK, Kachhwaha S, Kothari SL (2009) Synthesis of plant-mediated silver nanoparticles using papaya fruit extract and evaluation of their anti microbial activities. Dig J Nanomater Biostruct 4(3):557–563

Jain P, Pradeep T (2005) Potential of silver nanoparticle-coated polyurethane foam as an antibacterial water filter. Biotechnol Bioeng 90(1):59–63

Khan H, Khan MA, Abdullah (2015) Antibacterial, antioxidant and cytotoxic studies of total saponin, alkaloid and sterols contents of decoction of Joshanda: identification of components through thin layer chromatography. Toxicol Ind Health 31(3):202–8. https://doi.org/10.1177/0748233712468023. (**PMID: 23235996**)

Klebowski B, Depciuch J, Parlinska-Wojtan M, Baran J (2018) Applications of noble metal-based nanoparticles in medicine. Int J Mol Sci 19:4031. https://doi.org/10.3390/ijms19124031

Kumar P, Kizhakkedathu JN, Straus SK. (2018) Antimicrobial peptides: diversity, mechanism of action and strategies to improve the activity and biocompatibility in vivo. Biomol 19:8(1)

Moharekar S, Bora P, Kapre V, Uplane M, Daithankar V, Patil B, Moharekar S (2014) Exploitation of Aspergillus niger for synthesis of silver nanoparticles and their use to improve shelf life of fruits and toxic dye degradation. Int J Innovat Pharmaceut Sci Res 2(9):2106–2118

Moharrer S, Mohammadi B, Gharamohammadi RA, Yargoli M (2012) Biological synthesis of silver nanoparticles by Aspergillus flavus, isolated from soil of Ahar copper mine. Indian J Sci Technol 5(S3):2443–2444

Morones-Ramirez JR, Winkler JA, Spina CS, Collins JJ (2013) Silver enhances antibiotic activity against Gram-negative bacteria. Sci Transl Med. 5:190

Moutsiopoulou A, Broyles D, Dikici E, Daunert S, Deo SK. (2019) Molecular aptamer beacons and their applications in sensing, imaging, and diagnostics. Small 15(35):1902248

Nour S, Baheiraei N, Imani R, Khodaei M, Alizadeh A, Rabiee N et al (2019) A review of accelerated wound healing approaches: biomaterial-assisted tissue remodeling. J Mater Sci Mater Med 30:1–15. https://doi.org/10.1007/s10856-019-6319-6

Oliver S, Wagh H, Liang Y, Yang S, Boyer C (2018) Enhancing the antimicrobial and antibiofilm effectiveness of silver nanoparticles prepared by green synthesis. J Mater Chem B 6(24):4124–4138. https://doi.org/10.1039/c8tb00907d. (**Epub 2018 Jun 6 PMID: 32255155**)

Parashar V, Parashar R, Sharma B, Pandey AC (2009) Parthenium leaf extract mediated synthesis of silver nanoparticles: a novel approach towards weed utilization. Digest J Nanomater Biostruct (DJNB) 4:1

Rai MK, Deshmukh SD, Ingle AP, Gade AK (2012) Silver nanoparticles: the powerful nanoweapon against multidrug-resistant bacteria. J Appl Microbiol 112(5):841–852

Saigal, Irfan M, Khan P, Abid M, Khan MM (2019) Design, synthesis, and biological evaluation of novel fused spiro-4H-pyran derivatives as bacterial biofilm disruptor. ACS Omega 4:16794–16807

Tran QH, Le AT (2013) Silver nanoparticles: synthesis, properties, toxicology, applications and perspectives. Adv Nat Sci Nanosci Nanotechnol 4(3):20

Wang L, Hu C, Shao L (2017) The antimicrobial activity of nanoparticles: present situation and prospects for the future. Int J Nanomed 12:1227–1249. https://doi.org/10.2147/ijn.s121956